

FULL PAPER

A Semiempirical QM/MM Implementation and its Application to the Absorption of Organic Molecules in Zeolites

Timothy Clark¹, Alexander Alex², Bernd Beck¹, Peter Gedeck¹, and Harald Lanig¹

¹Computer-Chemie-Centrum des Instituts für Organische Chemie I, Friedrich-Alexander Universität Erlangen-Nürnberg, Nägelsbachstraße 25, D-91052 Erlangen, Germany. Tel. +49-9131-852 2948; Fax +49-9131-852 6565. E-mail: clark@organik.uni-erlangen.de

²Central Research, Pfizer Limited, Sandwich, Kent CT13 9NJ, United Kingdom

Received: 26 October 1998/ Accepted: 21 January 1999/ Published: 29 January 1999

Abstract An intermolecular hybrid semiempirical MO/molecular mechanics technique is described. The model allows polarisation of the quantum mechanical molecule(s), but not of the molecular mechanics part and is shown to be relatively insensitive to the size of the molecular mechanics environment. It has been validated by comparison of calculated and experimental absorption energies of small organic molecules in various zeolites. This validation gives us confidence that the method is also appropriate for experimentally less well characterised problems, such as solvation or ligand/enzyme complexation.

Keywords AM1, Semiempirical MO, Hybrid method, QM/MM, Zeolites, Absorption energies

Introduction

Quantum mechanical methods were originally developed to investigate small organic molecules. Semiempirical methods, for example have traditionally been used to calculate molecules of up to about 50 atoms. However, the rapid development of computational hardware and the efficiency of the MO software mean that now molecules up to about 500 atoms can be treated within standard semiempirical MO methods and complete proteins with localized MO [1] or divide and conquer techniques [2–4]. In order to be able to

investigate even larger molecular systems, several different approaches have been developed in the last few decades. In 1976, Warshel and Levitt presented the first mixed quantum mechanical/molecular mechanical (QM/MM) approach [5]. The basic idea of all QM/MM methods is to treat that part of the molecule that undergoes the most important electronic changes quantum mechanically and the rest of the system by molecular mechanics. Here, we distinguish between intramolecular methods, which often use so called ‘link atoms’, and pure intermolecular approaches. Many QM/MM techniques that combine different levels of QM methods with force fields have been published. Examples for methods using link atoms are those from Field, Bash and Karplus [6], Singh and Kollman [7], Merz and coworkers [8], Morokuma and Maseras [9] and Thiel and Bakowies [10]. The QM/MMpol approach by Thompson and coworkers is an example of a intermolecular QM/MM method [11].

Correspondence to: T. Clark

The authors like to thank Graham Richards for acting as guest editor.

We now report an implementation of an intermolecular QM/MM method with polarization of the QM component. In order to validate this approach, we have used it to calculate adsorption energies of small organic molecules in zeolites. Zeolites are microporous aluminosilicates that are widely used as industrial catalysts and for gas separation or ion exchange. Their catalytic properties are mainly influenced by the structure of the zeolite framework [12,13]. One of the important processes in catalysis is the adsorption of reactant and product molecules. Adsorption energies as well as the most favourable adsorption sites are often not known experimentally and therefore need to be calculated in order to understand the thermodynamics and sorption of substrates in zeolites. There have been many measurements of adsorption sites [14–16] and thermodynamic properties [17,18] of small molecules. Theoretical investigations focus on the treatment of diffusion processes because they play an essential role by e. g. favouring adsorption or transporting the reactants/products into/from the active site within the zeolite. Beside molecular dynamics simulations [19,20], Monte Carlo [21,22] and quantum-mechanical methods [23–26] are also frequently applied, the latter methods mainly on framework fragments. Ab-initio results for Brønsted acidity [27] of inorganic solids are much less advanced [28] than the accurate theoretical predictions for gas-phase molecules [29], but embedding zeolite models in a lattice of point charges improves the quality of the results significantly [30–32].

Semiempirical methods have also been used to calculate chemical reactions inside zeolites [33,34], but they are limited to problems up to around 500 atoms. Unit cells of for example zeolite ZSM-5, which is widely used as a cracking or methanol to gasoline (MTG) process catalyst [35], contain 288 framework atoms. Therefore, even semiempirical methods are not generally able to handle these zeolite systems [36]. We have therefore applied our QM/MM implementation to the interaction of small organic molecules (up to 20 atoms) with a given lattice of up to 23,040 point charges.

With this method it is possible to investigate adsorption in zeolite frameworks, structural changes in the guest molecules, and the calculation of chemical reactions paths including the characterisation of stationary points in the lattice.

Method

General Concept

The heat of adsorption of a molecule in a zeolite is the difference of the heat of formation of the molecule-zeolite complex, H_{M-Zeo} , and the sum of heat of formation of the isolated molecule H_M and the isolated zeolite, H_{Zeo} .

$$\Delta H_{ads} = H_{M-Zeo} - H_M - H_{Zeo} \quad (1)$$

A purely semiempirical calculation of the zeolite and the complex is not economical except for unacceptably small models of the zeolite. Therefore, we have divided the heat of formation of the complex further into

$$H_{M-Zeo} = H_{M,pert} + H_{Zeo,pert} + H_{M-Zeo,inter} \quad (2)$$

$H_{M,pert}$ is the heat of formation of the molecule influenced by the zeolite, $H_{zeo,pert}$ is the heat of formation of the zeolite under the influence of the molecule, and $H_{M-Zeo,inter}$ describes the interaction energy between the molecule and the zeolite.

As a first approximation, we further assume that the perturbation of the zeolite by the molecule can be neglected. Thus

$$H_{Zeo} = H_{Zeo,pert} \quad (3)$$

For the heat of adsorption we finally obtain,

$$\Delta H_{ads} = H_{M,pert} + H_{M-Zeo,inter} - H_M \quad (4)$$

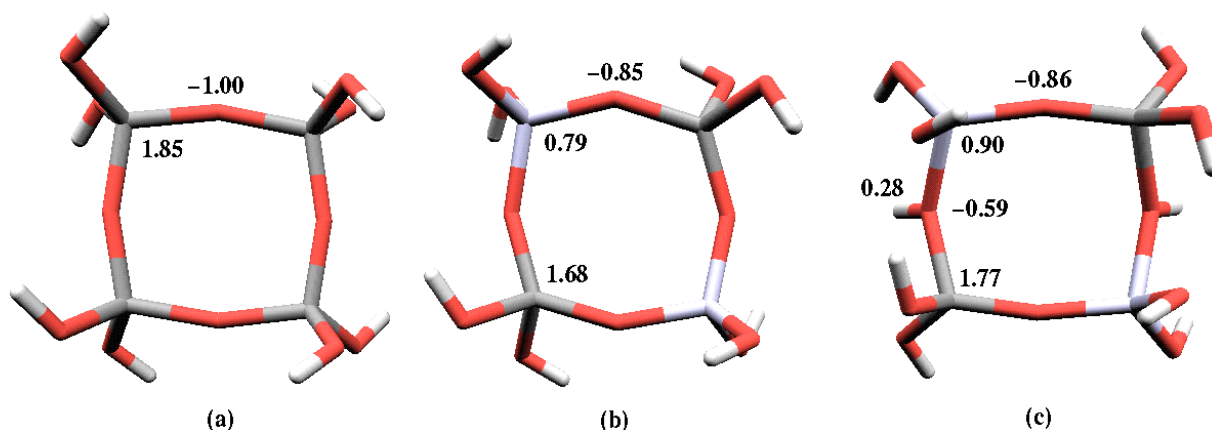


Figure 1 Zeolite models to derive reasonable charges for the point charge environment: (a) $[\text{SiO}(\text{OH})_2]_4$, (b) $[\text{SiO}(\text{OH})_2\text{AlO}(\text{OH})_2]_2$, and (c) $[\text{SiO}(\text{OH})_2\text{Al}(\text{OH})_3]_2$. All structures were fully optimised within C_2 symmetry using the AM1 hamiltonian

In our semiempirical treatment of the problem, we calculate the heat of formation of the unperturbed molecule *in vacuo*, H_M , using the conventional NDDO-based semiempirical MO-methods MNDO [37], AM1 [38] and PM3 [39]. To calculate $H_{M,pert}$, we include an additional term in the Fock matrix during the SCF procedure that describes the influence of the electrostatic potential of the zeolite. This and the method used to calculate the interaction energy $H_{M-zeo,inter}$ will be described below.

The electrostatic potential of the zeolite

The electrostatic potential of the zeolite environment is approximated by the electrostatic potential of point charges centred on the atoms of the zeolite. In order to obtain reasonable charges, we calculated small fragments of the zeolite framework using the AM1 hamiltonian in the semiempirical program package Vamp [40].

The results of these calculations for the three ring systems, $[\text{SiO}(\text{OH})_2]_4$, $[\text{SiO}(\text{OH})_2 \text{AlO}(\text{OH})_2]_2^{2-}$, and $[\text{SiO}(\text{OH})_2 \text{Al}(\text{OH})_3]_2$ are shown in Figure 1. From these results we derived average charges for O (-0.905), Al (0.847),

and Si (1.769) in zeolites. In the case of Broensted sites containing H-zeolites, a charge of -0.591 is assigned to the protonated oxygen and of 0.283 to the hydrogen.

Charges are assigned by the program. After the charges have been assigned, the total charge of the zeolite environment is determined. In order to avoid problems caused by the fact that we only treat a small fragment of the zeolite, we modify the charges of all oxygen atoms so that a total charge of zero is obtained. Usually, this only leads to changes in the order of 0.001 charge units per oxygen.

Perturbation of the QM part by the environment

In order to consider the electrostatic field of the zeolite environment during the SCF calculation, an additional one-electron term that describes the coulombic interaction between the electrons and the n_{MM} point charges q_i is added to the Fock matrix:

$$F(j) = F^0(j) + F^{pert}(j) = F^0(j) - \sum_{i=1}^{n_{MM}} \frac{q_i}{r_{ij}} \quad (5)$$

Figure 2 Benzene optimised within Silicalite (223 unit cells)

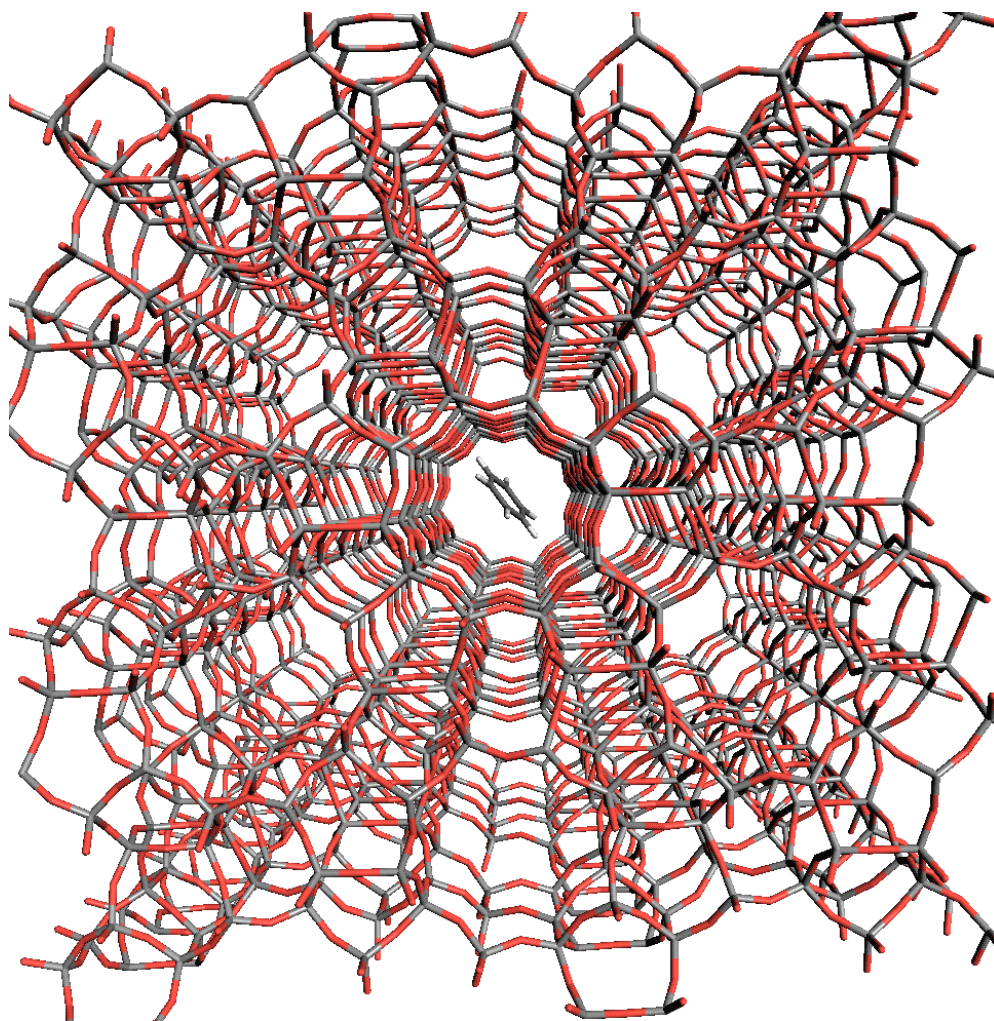


Table 1 Van der Waals radii (in Ångström) used in the point charge model

H	C	N	O	Al	Si
1.20	1.70	1.55	1.52	2.06	2.10

The corresponding Fock matrix F in the atomic orbital basis is given by:

$$F_{\mu\nu} = F_{\mu\nu}^0 - \sum_{i=1}^{n_{MM}} q_i \left\langle \mu \left| \frac{1}{r_{ij}} \right| \nu \right\rangle \quad (6)$$

The point charges are formally treated as s-orbitals with zero radius and the one-electron integrals substituted by two-centre two-electron integrals.

$$\left\langle \mu^{(\alpha)} \left| \frac{1}{r_{ij}} \right| \nu^{(\beta)} \right\rangle = \delta_{\alpha\beta} \left\langle \mu^{(\alpha)} s^i \left| \frac{1}{r_{ij}} \right| \nu^{(\beta)} s^i \right\rangle \quad (7)$$

The NDDO approximation restricts the additional one-electron integral to atomic orbitals that are on the same atom (indices μ , and ν). The remaining two-electron two-centre terms can now be calculated with a modification of the multipole approximation usually used in NDDO calculations [41].

$$\begin{aligned} \langle ss|ss \rangle &= \frac{1}{r} \\ \langle sp|ss \rangle &= \frac{1}{2|r+D_A|} - \frac{1}{2|r-D_A|} \\ \langle p_z p_z|ss \rangle &= \frac{1}{2r} + \frac{1}{4|r-2Q_A|} + \frac{1}{4|r+2Q_A|} \\ \langle p_x p_x|ss \rangle &= \frac{1}{2r} + \frac{1}{\sqrt{r^2 + 4Q_A^2}} \end{aligned} \quad (8)$$

Here, r is the distance between the atom and the point charge, D_A and Q_A are the usual semi-empirical parameters of the atom [37].

Calculation of the QM/MM interaction energies

For the QM/MM interaction energy $H_{M-zeo,inter}$ three contributions are considered.

- Electron - Point charge coulomb interaction E_{elec}
- Nucleus - Point charge coulomb interaction E_{nucl}
- van der Waals interaction E_{vdw}

Table 2 Parameters used for the calculation of the van der Waals energies in the point charge/van der Waals model

interaction type	well depth D_{ij} in kcal·mol ⁻¹
H-H	0.044
H-C	0.068
H-N	0.055
H-O	0.051
H-Al	0.149
H-Si	0.093 (0.133)*
C-C	0.105
C-N	0.085
C-O	0.079
C-Al	0.230
C-Si	0.101 (0.206)*
N-N	0.069
N-O	0.064
N-Al	0.187
N-Si	0.167
O-O	0.06
O-Al	0.174
O-Si	0.155

* Fitted to reproduce experimental data; original UFF values in parentheses

The total interaction energy is then,

$$H_{M-Zeo,inter} = E_{elec} + E_{nucl} + E_{vdw} \quad (9)$$

The coulomb interaction between the point charges and the electrons is calculated using the following expression.

$$E_{elec} = \sum_{i=1}^{n_{MM}} \sum_{j=1}^{n_{QM}} q_i^{PC} \sum_{\mu, \nu \in j} P_{\mu\nu} \left\langle \mu \left| \frac{1}{r_{ij}} \right| \nu \right\rangle \quad (10)$$

Here, q_i^{PC} is the charge of point charge i and P the density matrix elements. The integrals are calculated using the same approximation as used for the calculation of the Fock matrix perturbation.

The nucleus point charge coulomb interaction is calculated with

$$E_{nucl} = \sum_{i=1}^{n_{MM}} \sum_{j=1}^{n_{QM}} \frac{q_i^{PC} q_j^{nucl}}{r_{ij}} \quad (11)$$

To calculate the van der Waals interaction between the two systems a 6-12 Lennard-Jones potential is used.

$$E_{vdw} = \sum_{i=1}^{n_{MM}} \sum_{j=1}^{n_{QM}} D_{ij} \left[\left(\frac{a_{ij}^0}{r_{ij}} \right)^{12} - \left(\frac{a_{ij}^0}{r_{ij}} \right)^6 \right] \quad (12)$$

Table 3 Heat of formation ($\text{kcal}\cdot\text{mol}^{-1}$) for 18 molecules calculated in different sized Silicalite environments

	Silicalite model (No. of unit cells in each cartesian direction)						Mean	differ	Std dev	
	211	223	423	443	445	Min				Max
acetone	-62.97	-63.22	-63.47	-62.51	-62.97	-63.47	-62.51	-63.03	0.96	0.36
acetonitrile	9.33	8.82	8.60	9.92	9.12	8.60	9.92	9.16	1.32	0.51
benzene	8.55	8.56	8.26	8.86	8.63	8.26	8.86	8.57	0.60	0.21
butanol	-92.81	-92.41	-92.93	-91.85	-92.27	-92.93	-91.85	-92.45	1.08	0.44
1-butene	-12.65	-12.41	-12.69	-12.19	-12.38	-12.69	-12.19	-12.46	0.49	0.20
2-butyne	20.85	20.47	20.27	20.62	20.49	20.27	20.85	20.54	0.59	0.22
cyclopentane	-44.25	-45.00	-45.21	-44.85	-44.99	-45.21	-44.25	-44.86	0.96	0.37
ethane	-25.92	-26.36	-26.45	-26.31	-26.36	-26.45	-25.92	-26.28	0.53	0.21
ethanol	-75.33	-75.70	-76.00	-75.56	-75.58	-76.00	-75.33	-75.63	0.67	0.25
methane	-14.08	-14.29	-14.33	-14.25	-14.28	-14.33	-14.08	-14.25	0.26	0.10
methanol	-67.47	-67.16	-67.11	-67.10	-67.29	-67.47	-67.10	-67.23	0.37	0.16
n-butane	-44.79	-44.67	-44.83	-44.55	-44.65	-44.83	-44.55	-44.70	0.28	0.11
n-hexane	-62.38	-61.93	-62.17	-62.18	-62.33	-62.38	-61.93	-62.20	0.45	0.18
propanol	-83.81	-83.24	-83.36	-83.25	-83.27	-83.81	-83.24	-83.38	0.57	0.24
p-xylene	-9.06	-9.21	-9.35	-8.83	-8.91	-9.35	-8.83	-9.07	0.52	0.21
pyridine	17.83	17.67	17.51	17.78	17.69	17.52	17.83	17.70	0.32	0.12
toluene	-0.59	-0.47	-0.70	-0.33	-0.46	-0.70	-0.33	-0.51	0.38	0.14
water	-68.47	-68.06	-68.15	-68.42	-68.45	-68.47	-68.06	-68.31	0.40	0.19

The van der Waals radii a_{ij}^0 of the atoms taken from Bondi [42] are listed in Table 1. The well depth D_{ij} is calculated as the geometric mean of the single well depth potentials taken from the UFF force field [43]. For the calculations discussed below the well depth for Si-H, and Si-C interactions were changed from the original UFF values (see Table 2) to give better agreement with experiment.

Computational details

The method was implemented in the semiempirical program package Vamp [43]. The structures were fully optimised in the zeolite environment to a gradient norm of below $0.01 \text{ kcal } \text{\AA}^{-1}$ using the AM1 method. All semiempirical calculations were carried out on a SGI Power Challenge with two 195 MHz R10000 processors. The *ab initio* calculations were carried out on Convex and Cray mainframe computers.

Results

To test the performance and the reliability of the model, we studied a variety of molecule: zeolite complexes (see Tables 3 and 4). In a first step, the dependence of the calculated heats of formation on the size of the surrounding zeolite lattice was investigated. Five different silicalite fragments consisting of 211, 223, 423, 443, and 445 unit cells in the three spatial dimensions were created. Therefore, the smallest system had 576 and the largest 23,040 atoms in the lattice envi-

ronment. As an example, Figure 2 shows the optimised structure of benzene within the 223-Silicalite environment.

The position and structure of each test compound were fully optimised in the zeolite environment, the resulting heats of formation are shown in table 3.

As can be seen in Table 3, the dependence of the calculated heats of formation on the size of the environment is quite small. The fluctuations of the calculated heats of formation are for most compounds around $0.5 \text{ kcal}\cdot\text{mol}^{-1}$ ($0.26\text{--}0.67 \text{ kcal}\cdot\text{mol}^{-1}$). Larger differences were found for acetonitrile ($1.32 \text{ kcal}\cdot\text{mol}^{-1}$), butanol ($1.08 \text{ kcal}\cdot\text{mol}^{-1}$), acetone ($0.96 \text{ kcal}\cdot\text{mol}^{-1}$) and cyclopentane ($0.96 \text{ kcal}\cdot\text{mol}^{-1}$). The corresponding standard deviations range between $0.10 \text{ kcal}\cdot\text{mol}^{-1}$ for methane and $0.51 \text{ kcal}\cdot\text{mol}^{-1}$ for acetonitrile. These results show that the method is almost independent on the size of the environment.

The following examples indicate the calculational times used by the QM/MM method. For water the total time used (195 MHz R10000) was between 2.4 s for the small (211) Silicalite and 31.2 s for the large (445) one. In the case of pyridine 42 s (211) and 938 s (445) are necessary to complete the calculations.

As a second test the model was used to calculate the heats of adsorption for 21 different organic molecules in 4 zeolites (31 test combinations). The values obtained are shown in table 4 and plotted against experimental heats of adsorption in figure 3.

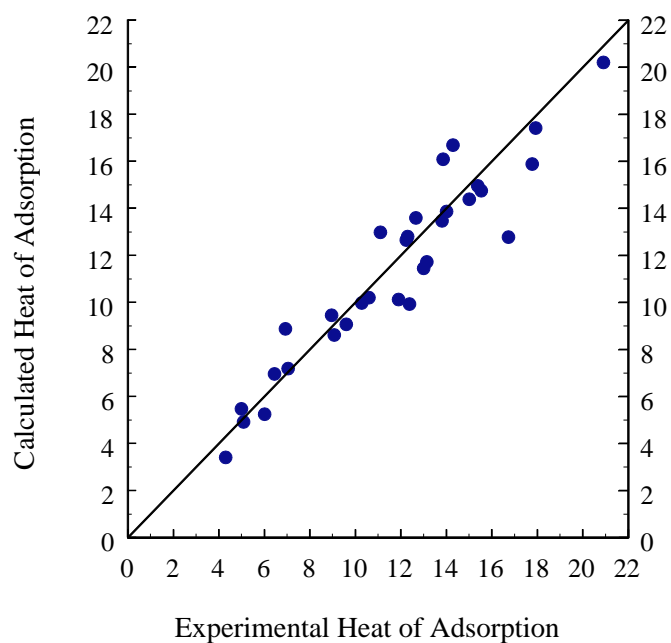
The resulting correlation coefficient is 0.95 with a standard deviation of $1.36 \text{ kcal}\cdot\text{mol}^{-1}$. The largest deviations between calculated and experimental heats of adsorption occur for benzene in ZSM-5 ($3.95 \text{ kcal}\cdot\text{mol}^{-1}$), cyclohexane in X

Table 4 Comparison of experimental and calculated heats of adsorption (in kcal·mol⁻¹) for 21 different organic molecules in four different zeolites to give 31 test compounds

molecule	zeolite	ΔH_{exp}	ΔH_{calc}^*	ΔE
acetone	Silicalite	14.01 [46]	13.87	0.14
acetonitrile	Silicalite	11.90 [46]	10.13	1.77
benzene	Silicalite	13.81 [46]	13.47	0.34
benzene	ZSM-5	16.73 [46]	12.78	3.95
butanol	Silicalite	14.30 [16]	16.70	2.40
1-butene	Silicalite	12.24 [14]	12.65	0.41
2-butyne	Silicalite	13.01 [15]	11.45	1.56
cyclohexane	X	12.38 [14]	9.93	2.45
cyclopentane	Silicalite	13.86 [14]	16.09	2.23
ethane	A	6.02 [44]	5.25	0.77
ethane	X	5.09 [14]	4.92	0.17
ethane	Silicalite	6.93 [14]	8.88	1.95
ethane	ZSM-5	8.96 [14]	9.46	0.50
ethanol	Silicalite	11.10 [16]	12.98	1.88
methane	A	4.30 [14]	3.42	0.88
methane	Silicalite	5.00 [14]	5.48	0.48
methanol	Silicalite	10.60 [16]	10.21	0.39
n-butane	X	9.08 [14]	8.61	0.47
n-butane	Silicalite	12.67 [14]	13.60	0.93
n-butane	ZSM-5	15.54 [14]	14.75	0.79
n-hexane	X	13.15 [14]	11.72	1.43
n-hexane	Silicalite	17.93 [14]	17.42	0.51
n-pentane	X	10.28 [14]	9.97	0.31
propane	A	7.05 [44]	7.19	0.14
propane	X	6.45 [14]	6.97	0.52
propanol	Silicalite	12.30 [16]	12.81	0.51
pyridine	Silicalite	15.01 [46]	14.39	0.62
p-xylol	Silicalite	17.78 [47]	15.89	1.89
p-xylol	ZSM-5	20.91 [47]	20.21	0.70
toluol	Silicalite	15.39 [47]	14.95	0.44
water	Silicalite	9.60 [48]	9.07	0.53

* For all compounds calculated in Silicalite the mean values from table 3 were used

Figure 3 Plot of experimental vs calculated heats of adsorption (kcal·mol⁻¹). The line shown is the 1:1 line (perfect agreement), not the least squares fit



(2.45 kcal·mol⁻¹), butanol in Silicalite (2.40 kcal·mol⁻¹) and cyclopentane in Silicalite (2.23 kcal·mol⁻¹).

For the remaining 27 test compounds 6 have deviations from experiment between 1.43 kcal·mol⁻¹ and 1.95 kcal·mol⁻¹ and for 21 the differences range between 0.14 kcal·mol⁻¹ and 0.93 kcal·mol⁻¹.

Conclusion

The simple QM/MM model presented here has been validated using heats of adsorption in zeolites. The results are encouraging and suggest that the computationally effective strategy of only allowing polarisation of the QM substrate can give good results. The accuracy of the calculated absorption energies, which are experimentally well known, gives us some confidence that the same technique applied to ligand/enzyme interactions, where validation data is very sparse, should also give good results. Initial docking studies are in progress. The model reported here is now being extended to allow optimisation of the MM environment and intramolecular QM/MM calculations.

Acknowledgement This work was supported by the Deutsche Forschungsgemeinschaft, Oxford Molecular Limited, Pfizer Limited and the Fonds der Chemischen Industrie. We thank B. J. Teppen for providing us with cartesian coordinates of the zeolite unit cells.

References

- Stewart, J. J. P. *Int. J. Quant. Chem.* **1996**, *58*, 133.
- Zhao, Q.; Yang, W. *J. Chem. Phys.* **1995**, *102*, 9598.
- Yang, W.; Lee, T.-S. *J. Chem. Phys.* **1995**, *103*, 5674.
- Dixon, S. L.; Merz, Jr., K. M. *J. Phys. Chem.* **1996**, *104*, 6643.
- Warshel, A.; Levitt, M. *J. Mol. Biol.* **1976**, *103*, 227.
- Field, M. J.; Bash, P. A.; Karplus, M. *J. Comput. Chem.* **1990**, *11*, 700.
- Singh, U. C.; Kollman, P. A. *J. Comput. Chem.* **1986**, *7*, 718.
- Stanton, R. V.; Hartsough, D. S.; Merz, Jr., K. M. *J. Comput. Chem.* **1996**, *16*, 113.
- Maseras, F.; Morokuma, K. *J. Comput. Chem.* **1995**, *16*, 1170.
- Bakowies, D.; Thiel, W. *J. Phys. Chem.* **1996**, *100*, 10580.
- Thompson, M. A.; Schenter, G. K. *J. Phys. Chem.* **1995**, *99*, 6374.
- Breck, D. W. *Zeolite Molecular Sieves*, Wiley, New York, **1974**.
- Modelling of Structure and Reactivity in Zeolites, Catlow, C. R. A. (Ed.), Academic Press, London, **1992**.
- Stach, H.; Lohse, U.; Thamm, H.; Schirmer, W. *Zeolites* **1986**, *6*, 74.
- Shen, D.; Rees, L. V. C. *Zeolites* **1991**, *11*, 684.
- Nayak, V. S.; Moffat, J. B. *J. Phys. Chem.* **1988**, *92*, 7097.
- Sun, M. S.; Shah, D. B.; Xu, H. H.; Talu, O. *J. Phys. Chem. B* **1998**, *102*, 1466.
- Olson, D. H.; Reischman, P. T. *Zeolites* **1996**, *17*, 434.
- Demontis, P.; Suffritti, G. B. *Chem. Rev.* **1997**, *97*, 2845.
- Kantola, J.; Vaara, J.; Rantala, T.; Jokisaari, J. *J. Chem. Phys.* **1997**, *107*, 6470.
- Pellenq, R. J.-M.; Nicholson, D. *Langmuir* **1995**, *11*, 1626.
- Smit, B. *J. Phys. Chem.* **1995**, *99*, 5597.
- Sauer, J.; Horn, H.; Haeser, M.; Ahlrichs, R. *Chem. Phys. Lett.* **1990**, *173*, 26.
- Sauer, J. *Chem. Rev.* **1989**, *89*, 199.
- Derouane, E. G.; Fripiat, J. G.; von Ballmoos, R. *J. Phys. Chem.* **1990**, *94*, 1687.
- Shah, R.; Gale, J. D.; Payne, M. C. *J. Phys. Chem.* **1996**, *100*, 11688.
- Sierka, M.; Eichler, U.; Datka, J.; Sauer, J. *J. Phys. Chem. B* **1998**, *102*, 6397.
- Brändle, M.; Sauer, J. *J. Am. Chem. Soc.* **1998**, *120*, 1556.
- Curtiss, L. A.; Raghavachari, K.; Trucks, G. W.; Pople, J. A. *J. Chem. Phys.* **1991**, *94*, 7221.
- Sauer, J. in Ref. 13, p. 204.
- Allavena, M.; Kassab, E. *Solid State Ionics* **1993**, *61*, 33.
- Greatbanks, S. P.; Sherwood, P.; Hillier, I. H. *J. Phys. Chem.* **1994**, *98*, 8134.
- Farnworth, K. J.; O'Malley, P. J. *Electron. J. Theor. Chem.* **1996**, *1*, 172.
- Chatterjee, A.; Vetrivel, R. *J. Chem. Soc., Faraday Trans.* **1995**, *91*, 4313.
- Olson, D. H.; Kokotallo, G. T.; Lawton, S. L.; Meier, W. M. *J. Phys. Chem.* **1981**, *85*, 2238 and references therein.
- Meier, W. M.; Olson, D. H.; Baerlocher, Ch. *Atlas of Zeolite Structure Types*, 4th revised edition, Elsevier, London, **1996**.
- Dewar, M. J. S.; Thiel, J. *J. Am. Chem. Soc.* **1977**, *99*, 4899.
- Dewar, M. J. S.; Zoebisch, E. G.; Healy, E. F.; Stewart, J. J. P. *J. Am. Chem. Soc.* **1985**, *107*, 3902.
- a) Stewart, J. J. P. *J. Comp. Chem.* **1989**, *10*, 209.
b) Stewart, J. J. P. *J. Comp. Chem.* **1989**, *10*, 221.
- Clark, T.; Alex, A.; Beck, B.; Chandrasekhar, J.; Gedeck, P.; Horn, A.; Hutter, M.; Rauhut, G.; Sauer, W.; Steinke, T. *Vamp 7.0* (Oxford Molecular Group, Oxford, 1998).
- Dewar, M. J. S.; Thiel, W. *Theor. Chim. Acta* **1977**, *46*, 89.
- Bondi, A. *J. Phys. Chem.* **1964**, *68*, 441.
- Rappé, A. K.; Casewit, C. J.; Colwell, K. S.; Goddard III, W. A.; Stiff, W. M. *J. Am. Chem. Soc.* **1992**, *114*, 10024.
- Yasuda, Y.; Suzuki, Y.; Fukuda, H. *J. Phys. Chem.* **1991**, *95*, 2486.
- Richards, R. E.; Rees, L. V. C. *Zeolites* **1988**, *8*, 35.
- Thamm, H. *J. Phys. Chem.* **1988**, *92*, 193.
- Pope, C. G. *J. Phys. Chem.* **1986**, *90*, 835.
- Vigné-Maeder, F.; Auroux, A. *J. Phys. Chem.* **1990**, *94*, 316.